

# Reduced Expression for Timber Structure with Flexible Horizontal Diaphragm and Seismic Response Evaluation Method

Y. Yamazaki, K. Kasai & H. Sakata

Tokyo Institute of Technology, Japan



## SUMMARY:

This paper discusses various effects of horizontal diaphragm flexibility on dynamic properties and seismic responses of timber structure. Equations of motion of a building with multiple discretized diaphragm elements are derived by defining reduced degrees of freedom. A method to predict seismic responses is proposed by using the reduced degrees of freedom, and example structures are used to demonstrate its accuracy and advantages. Modification of the method to rationalize and improve the conventional method is also discussed, by indicating good accuracy except when horizontal diaphragm is very flexible and stiffness eccentricity is large. Finally, Application of the method to multi-span structure more than 3-span is also demonstrated.

*Keywords: Rigid floor, Flexible floor, Horizontal diaphragm, Dynamic properties, Timber houses*

## 1. INTRODUCTION

All the elements resisting horizontal forces should be connected with stiff and strong floor diaphragm in terms of seismic resistance. Additionally, rigid floor is necessary to analyze seismic behavior of structure using simplified model such as multi-mass model with shear spring. Therefore, seismic design codes in many countries are based on “rigid floor assumption”.

However, floor diaphragm of Japanese timber structures may not be stiff enough to satisfy rigid floor assumption. The relation between floor stiffness and dynamic properties of system has been studied through many experiments and analyses of 3-dimensional frame model. Kawai (2000) studied applicability of equivalent linearization method for evaluating seismic response of timber structure with plywood shear walls and flexible floor diaphragm. The study showed that the prediction had good accuracy except when stiffness eccentricity was large because the method considered equally distributed inertial force. Conventional methods do not seem to have enough accuracy because theoretical approach is lacked. Therefore, evaluation method of dynamic properties considering floor flexibility is required.

In Japan, floor diaphragm usually consists of timber panels fastened to floor frame with nails. Since connections of timber structure are like pin joints, floor frame deforms keeping parallelogram. Considering above behavior of timber structure, the authors have already presented dynamics-based approach for 1-span model, which is able to consider exact distribution of inertial force and displacement mode subjected to uni-directional earthquake (Yamazaki et al. 2011). The theory gives dynamic properties using some familiar properties of structure.

The objective of this research is to extend the theory to 2-span model and present reduced expression for timber structure with flexible floor diaphragm. How to determine criteria for “rigid floor” is also discussed using key parameters derived from equation of motion. Finally, proposed method is applied to multi-span structure more than 3-span, and its validity and advantage are demonstrated.

## 2. EQUATION OF MOTION

### 2.1. Considered Model

As shown in **Figure 1**, 2-span single story model with multiple discretized diaphragm elements subjected to  $x$ -directional input motion is considered. Three springs and dashpots in each direction represent frames or walls. Floor diaphragm is divided to four areas ; Area11, Area12, Area21 and Area22, respectively.

If each area acts like shear panel, displacement mode of structure is defined as shown in **Figure 2**. Components of rigid body which does not includes shear deformation of floor diaphragm are  $u_x$  and  $\theta$ . These are displacement of center of mass ( $c.m.$ ) in  $x$ -direction and rotation around  $c.m.$ , respectively. Other components are attributed to shear deformation of floor diaphragm ;  $\gamma_{x1}$ ,  $\gamma_{x2}$ ,  $\gamma_{y1}$  and  $\gamma_{y2}$ , respectively. These are selected in condition that  $\gamma_{x1} + \gamma_{x2} - \gamma_{y1} - \gamma_{y2}$  equals to zero, which means shear forces do not rotate floor diaphragm.

If bilaterally symmetric structure is considered,  $\gamma_{y1} = \gamma_{y2} (= \gamma_y)$  is derived. Moreover,  $u_x$ ,  $(\theta + \gamma_{x1})$ ,  $(\theta + \gamma_{x2})$  and  $(\theta - \gamma_y)$  are dominant parameters to express motion of structure. As a result, it is found that the structure can be dealt with 4-degree of freedom system.

Besides, beams are likely to affect stiffness element of floor diaphragm. For example, if  $\gamma_{x1}$  does not equal to  $\gamma_{x2}$ , beams must be bent around their weak axes. Aoki et al. (2002) have reported that bending stiffness of beams is likely to affect total stiffness of floor diaphragm especially when floor shear stiffness is low. Owing to this, rotational springs are added in boundary of each area as shown in **Figure 3**, which represent bending of beams and output moment proportional to  $(\gamma_{x1} - \gamma_{x2})$ .

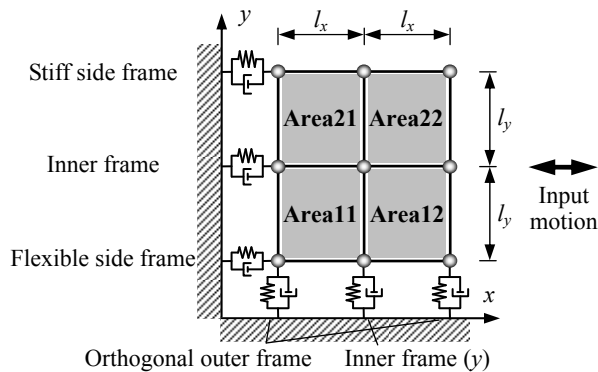
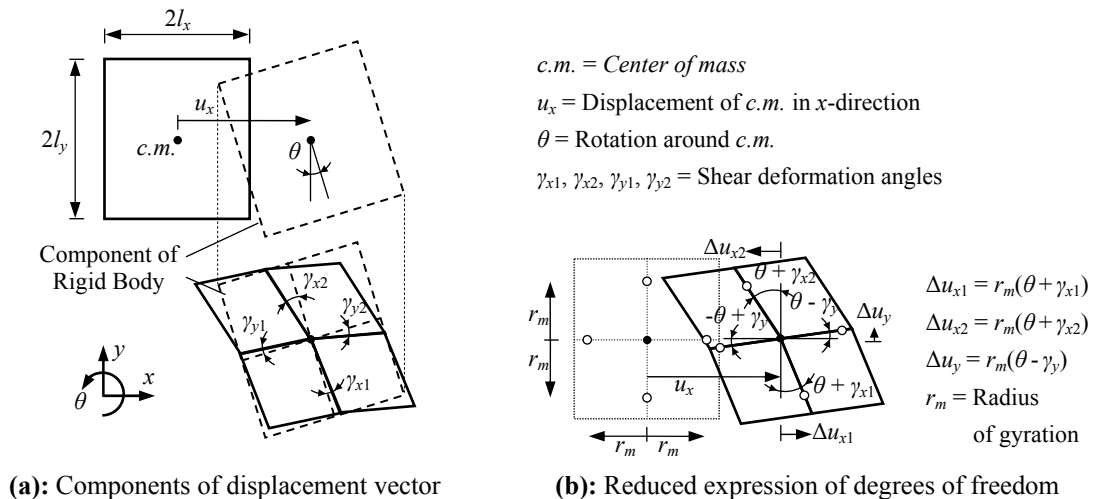


**Figure 1:** Considered model



**(a):** Components of displacement vector

**(b):** Reduced expression of degrees of freedom

**Figure 2:** Displacement mode

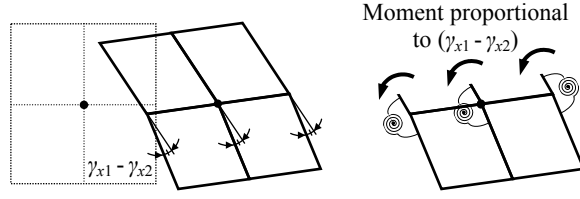


**Figure 3:** Rotational springs representing bending of beams around weak axis

## 2.2. Equilibrium of Force in An Area

**Figure 4** shows an example of equilibrium of force in Area11. 1) Total force and moment of stiffness elements in Area11, 2) Inertial force, 3) Shear forces transmitted from adjacent panels and 4) Bending moment of beams are taken into account. Coordinate of stiffness element and mass element in Area  $ij$  is defined in its local coordinate system as shown in **Figure 5**, and the following parameters are calculated.

$$K_{xij} = \sum_l k_{xij}^{(l)}, \quad K_{\theta ij} = \sum_l \left[ k_{xij}^{(l)} (y_{ij}^{(l)})^2 + k_{yij}^{(l)} (x_{ij}^{(l)})^2 \right], \quad e_{yij} = \sum_l k_{xij}^{(l)} y_{ij}^{(l)} / K_{xij} \quad (2.1a-c)$$

$$m_0 = \sum_l m_{ij}^{(l)}, \quad I_0 = \sum_l m_{ij}^{(l)} \left[ (x_{mij}^{(l)})^2 + (y_{mij}^{(l)})^2 \right] \quad (2.2a,b)$$

Where,  $k_{xij}^{(l)}, k_{yij}^{(l)}$  = stiffness of  $l$ -th element in  $x$ - and  $y$ - direction, respectively.  $x_{ij}^{(l)}, y_{ij}^{(l)}$  = Coordinate of  $l$ -th stiffness element.  $m_{ij}^{(l)}$  = mass of  $l$ -th element.  $x_{mij}^{(l)}, y_{mij}^{(l)}$  = Coordinate of  $l$ -th mass element. Eqn. 2.1a-c show total stiffness, rotational stiffness and stiffness eccentricity in Area  $ij$ , respectively.

When the model is subjected to ground acceleration  $\ddot{u}_g$ , Equilibrium of force in Area  $ij$  are described as follows.

$$\begin{aligned} m_0 [\ddot{u}_x + (l_y/2)(\ddot{\theta} + \ddot{\gamma}_{x1}) + \ddot{u}_g] + K_{x11} [u_x + (l_y/2)(\theta + \gamma_{x1})] - K_{x11} e_{y11} [\theta + \gamma_{x1}] + Q_{x1} &= 0 \\ -m_0 (l_x/2)(\ddot{\theta} - \ddot{\gamma}_y) - K_{y11} (l_x/2)(\theta - \gamma_y) + Q_{y1} &= 0 \\ I_0^{(x)} (\ddot{\theta} + \ddot{\gamma}_{x1}) + I_0^{(y)} (\ddot{\theta} - \ddot{\gamma}_y) - K_{x11} e_{y11} [u_x + (l_y/2)(\theta + \gamma_{x1})] + K_{\theta 11}^{(x)} (\theta + \gamma_{x1}) \\ + K_{\theta 11}^{(y)} (\theta - \gamma_y) - Q_{x1} (l_y/2) + Q_{y1} (l_x/2) + K_{\theta b} (\gamma_{x1} - \gamma_{x2})/2 &= 0 \\ I_0^{(x)} (\ddot{\theta} + \ddot{\gamma}_{x1}) - K_{x11} e_{y11} [u_x + (l_y/2)(\theta + \gamma_{x1})] \\ + K_{\theta 11}^{(x)} (\theta + \gamma_{x1}) - Q_{x1} (l_y/2) - K_{\theta b} (\gamma_{x1} - \gamma_{x2})/2 &= -GV_0 (\gamma_{x1} + \gamma_y) \\ I_0^{(y)} (\ddot{\theta} - \ddot{\gamma}_y) + K_{\theta 11}^{(y)} (\theta - \gamma_y) + Q_{y1} (l_x/2) &= GV_0 (\gamma_{x1} + \gamma_y) \end{aligned} \quad (2.3a-e)$$

Where, the following parameters are added.

$$K_{\theta ij}^{(x)} = \sum_l k_{xij}^{(l)} (y_{ij}^{(l)})^2, \quad K_{\theta ij}^{(y)} = \sum_l k_{yij}^{(l)} (x_{ij}^{(l)})^2 \quad (2.4a,b)$$

$$I_0^{(x)} = \sum_l m_{ij}^{(l)} (y_{mij}^{(l)})^2 (= m_0 l_y^2 / 12), \quad I_0^{(y)} = \sum_l m_{ij}^{(l)} (x_{mij}^{(l)})^2 (= m_0 l_x^2 / 12) \quad (2.5a,b)$$

These satisfy  $K_{\theta ij} = K_{\theta ij}^{(x)} + K_{\theta ij}^{(y)}$  and  $I_0 = I_0^{(x)} + I_0^{(y)}$ . The right member of Eqn. 2.5 is satisfied only when mass is equally distributed.  $G, V_0$  = shear modulus and volume when floor diaphragm of each area is assumed to be elastic plate.  $K_{\theta b}$  = Rotational stiffness of spring located in connection between

lower areas (i.e. Area11 and Area12) and upper areas (i.e. Area21 and Area22).  $Q_{x1}$ ,  $Q_{y1}$  = shear forces transmitted from adjacent panels, which are not shown in equilibrium of total area because these are internal forces of floor diaphragm.

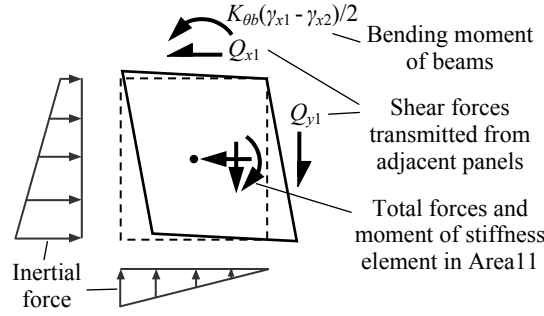


Figure 4: External forces applied to panel of Area11

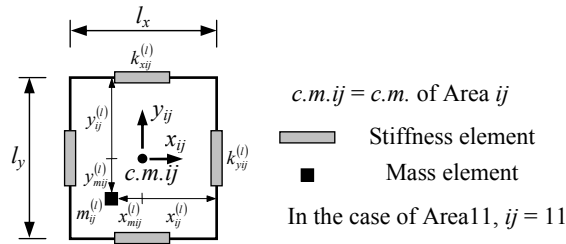


Figure 5: Coordinate of stiffness element and mass element in Area  $ij$

### 2.3. Equilibrium of Force in Total Area

By considering equilibrium of force in all areas and setting origin in center of mass, equation of motion is obtained as follows.

$$\begin{aligned}
 & \begin{bmatrix} m & ml_y/4 & -ml_y/4 & 0 \\ & I^{(x)}/2 & 0 & 0 \\ & & I^{(x)}/2 & 0 \\ \text{sym.} & & & I^{(y)} \end{bmatrix} \begin{Bmatrix} \ddot{u}_x \\ \ddot{\theta} + \ddot{\gamma}_{x1} \\ \ddot{\theta} + \ddot{\gamma}_{x2} \\ \ddot{\theta} - \ddot{\gamma}_y \end{Bmatrix} \\
 & + \begin{bmatrix} K_x & -e_{y1}K_{x1} & -e_{y2}K_{x2} & 0 \\ & K_{\theta 1}^{(x)} + GV/2 + K_{\theta b} & -K_{\theta b} & -GV/2 \\ & & K_{\theta 2}^{(x)} + GV/2 + K_{\theta b} & -GV/2 \\ \text{sym.} & & & K_{\theta}^{(y)} + GV \end{bmatrix} \begin{Bmatrix} u_x \\ \theta + \gamma_{x1} \\ \theta + \gamma_{x2} \\ \theta - \gamma_y \end{Bmatrix} \\
 & = \begin{bmatrix} m & ml_y/4 & -ml_y/4 & 0 \\ & I^{(x)}/2 & 0 & 0 \\ & & I^{(x)}/2 & 0 \\ \text{sym.} & & & I^{(y)} \end{bmatrix} \begin{Bmatrix} 1 \\ 0 \\ 0 \\ 0 \end{Bmatrix} \ddot{u}_g
 \end{aligned} \tag{2.6}$$

Where, we use  $m = 4m_0$  and  $V = 4V_0$ , and the following parameters of global coordinate system are also defined.

$$I^{(x)} = 4I_0^{(x)} + 4m_0(l_y/2)^2, \quad I^{(y)} = 4I_0^{(y)} + 4m_0(l_x/2)^2 \tag{2.7a,b}$$

$$K_{x1} = K_{x11} + K_{x12}, \quad K_{x2} = K_{x21} + K_{x22} \tag{2.8a,b}$$

$$e_{y1} = \left[ (K_{x11}e_{y11} + K_{x12}e_{y12}) - K_{x1}(l_y/2) \right] / K_{x1} \quad (2.9a,b)$$

$$e_{y2} = \left[ (K_{x21}e_{y21} + K_{x22}e_{y22}) + K_{x2}(l_y/2) \right] / K_{x2}$$

$$K_{\theta 1}^{(x)} = K_{\theta 11}^{(x)} + K_{\theta 12}^{(x)} - 2(K_{x11}e_{y11} + K_{x12}e_{y12})(l_y/2) + (K_{x11} + K_{x12})(l_y/2)^2$$

$$K_{\theta 2}^{(x)} = K_{\theta 21}^{(x)} + K_{\theta 22}^{(x)} + 2(K_{x21}e_{y21} + K_{x22}e_{y22})(l_y/2) + (K_{x21} + K_{x22})(l_y/2)^2 \quad (2.10a-c)$$

$$K_{\theta}^{(y)} = K_{\theta 21}^{(y)} + K_{\theta 22}^{(y)} + K_{\theta 21}^{(y)} + K_{\theta 22}^{(y)} + (K_{y11} + K_{y12} + K_{y21} + K_{y22})(l_x/2)^2$$

In Eqn. 2.8-2.10, index “1” and “2” mean that the parameter is defined in “lower areas” and “upper areas”, respectively. Hence, the following relations are satisfied.

$$K_x = K_{x1} + K_{x2} \quad , \quad K_{\theta} = K_{\theta 1}^{(x)} + K_{\theta 2}^{(x)} + K_{\theta}^{(y)} \quad , \quad e_y = (K_{x1}e_{y1} + K_{x2}e_{y2}) / K_x \quad (2.11a-c)$$

These three parameters are commonly-used for structure with rigid diaphragm.

## 2.4. Normalization of Equation of Motion

In this section, parameters in equation of motion are normalized instead of physical parameters. At first, the followings are defined.

$$\omega_x = \sqrt{K_x/m} \quad , \quad \omega_{\theta} = \sqrt{K_{\theta}/I} \quad (2.12a,b)$$

Where,  $\omega_x$ ,  $\omega_{\theta}$  = natural circular frequency of the structure assuming its rotation/translation is fixed, respectively. In addition, the following coordinate conversions are conducted.

$$\Delta u_{x1} = r_m(\theta + \gamma_{x1}) \quad , \quad \Delta u_{x2} = r_m(\theta + \gamma_{x2})$$

$$\Delta u_y = r_m(\theta - \gamma_y) \quad , \quad r_m = \sqrt{I/m} \quad \left( = \sqrt{(l_x^2 + l_y^2)/3} \right) \quad (2.13a-d)$$

Where,  $r_m$  = radius of gyration,  $I$  = moment of inertia. The right member of Eqn. 2.13d is satisfied only when mass is equally distributed. Using above parameters, Eqn. 2.6 is converted as follows.

$$\mathbf{m}\ddot{\mathbf{u}} + \mathbf{k}\mathbf{u} = -\mathbf{m}\{\mathbf{1}\}\ddot{u}_g \quad (2.14)$$

$$\mathbf{m} = \begin{bmatrix} 1 & l_y/4r_m & -l_y/4r_m & 0 \\ & (1+\alpha)/4 & 0 & 0 \\ & & (1+\alpha)/4 & 0 \\ sym. & & & (1-\alpha)/2 \end{bmatrix} \quad , \quad \mathbf{u} = \begin{Bmatrix} u_x \\ \Delta u_{x1} \\ \Delta u_{x2} \\ \Delta u_y \end{Bmatrix} \quad , \quad \{\mathbf{1}\} = \begin{Bmatrix} 1 \\ 0 \\ 0 \\ 0 \end{Bmatrix}$$

$$\mathbf{k} = \omega_x^2 \begin{bmatrix} 1 & -\bar{e}_{y1} \frac{K_{x1}}{K_x} & -\bar{e}_{y2} \frac{K_{x2}}{K_x} & 0 \\ \frac{\omega_{\theta}^2}{\omega_x^2} \left( \cos^2 \psi_{x1} \frac{K_{\theta 1}}{K_{\theta}} + \frac{\omega_r^2}{8\omega_{\theta}^2} + \frac{\omega_b^2}{\omega_{\theta}^2} \right) & -\frac{\omega_{\theta}^2 \omega_b^2}{\omega_x^2 \omega_{\theta}^2} & -\frac{\omega_{\theta}^2 \omega_r^2}{\omega_x^2 8\omega_{\theta}^2} & \\ \frac{\omega_{\theta}^2}{\omega_x^2} \left( \cos^2 \psi_{x2} \frac{K_{\theta 2}}{K_{\theta}} + \frac{\omega_r^2}{8\omega_{\theta}^2} + \frac{\omega_b^2}{\omega_{\theta}^2} \right) & -\frac{\omega_{\theta}^2 \omega_b^2}{\omega_x^2 \omega_{\theta}^2} & -\frac{\omega_{\theta}^2 \omega_r^2}{\omega_x^2 8\omega_{\theta}^2} & \\ sym. & & & \frac{\omega_{\theta}^2}{\omega_x^2} \left( \sin^2 \psi_x + \frac{\omega_r^2}{4\omega_{\theta}^2} \right) \end{bmatrix} \quad (2.15a-d)$$

Where,

$$\bar{e}_{y1} = e_{y1}/r_m \quad , \quad \bar{e}_{y2} = e_{y2}/r_m$$

$$\cos^2 \psi_{x1} = K_{\theta 1}^{(x)}/K_{\theta 1} \quad , \quad \sin^2 \psi_{x1} = K_{\theta 1}^{(y)}/K_{\theta 1} \quad (2.16a,b)$$

$$\cos^2 \psi_{x2} = K_{\theta 2}^{(x)} / K_{\theta 2} \quad , \quad \sin^2 \psi_{x2} = K_{\theta 2}^{(y)} / K_{\theta 2} \quad , \quad \sin^2 \psi_x = K_{\theta}^{(y)} / K_{\theta} \quad (2.17a-e)$$

$$\omega_y = \sqrt{4GV/I} \quad , \quad \omega_b = \sqrt{K_{\theta b}/I} \quad , \quad \alpha = (I^{(x)} - I^{(y)})/I \quad (2.18a-c)$$

$\omega_y$  and  $\omega_b$  means floor stiffness against shear and bending, respectively. Since their units are the same as those of circular frequency, “ $\omega$ ” is used. In the stiffness matrix (Eqn. 2.15d), stiffness of floor diaphragm is expressed in nondimensional parameters ;  $\omega_y/\omega_{\theta}$  for shear and  $\omega_b/\omega_{\theta}$  for bending, respectively.

### 3. DETERMINATION OF PARAMETERS

In this paper, we focus on the effects of not only floor flexibility but also stiffness eccentricity. As shown in **Figure 6**, two types of model with different stiffness balance are considered. These models have nearly the same eccentric ratio  $R_{ex}$  which is used in Japanese Building Standard Law.  $R_{ex}$  means vulnerability to torsion, and it is calculated as follows.

$$R_{ex} = \frac{e_y}{\sqrt{(K_{\theta}/K_x) - e_y^2}} \quad (3.1)$$

As for design of timber houses in Japan,  $R_{ex}$  must be lower than 0.3.  $R_{ex}$  of model 1 and model 2 are about 0.3.

Another characteristic of this research is consideration of bending stiffness of floor diaphragm. As mentioned by Aoki et al. (2002), the effect should not be neglected especially in the case of quite flexible floor diaphragm. In this study, bending flexibility is simulated considering ideal rotational spring, and how to determine its stiffness is explained as follows.

As shown in **Figure 7**, simple beam and rigid link system are considered. When deflection of the two models are the same, we can obtain  $K_{\theta b} = 3EI/(2l_y)$ . Where,  $E$  = Young’s modulus of beam,  $I$  = moment of inertia of beam around weak axis. However, we can not exactly evaluate  $I$  because wood panels are typically fastened to beams with nails. Therefore,  $E = 8$  kN/mm and  $l_y = 3.64$  m are assumed, and two cases of  $I$  ( =  $(240 \cdot 120^3/12) \cdot 3$ ,  $(240 \cdot 120^3/12) \cdot 3 \cdot 10$  ) are considered. The former means that there are three usual beams ( $K_{\theta b} = 342$  kNm/rad), and the latter is ten times of it ( $K_{\theta b} = 3420$  kNm/rad). These are described as “low bending stiffness” and “high bending stiffness”, respectively.

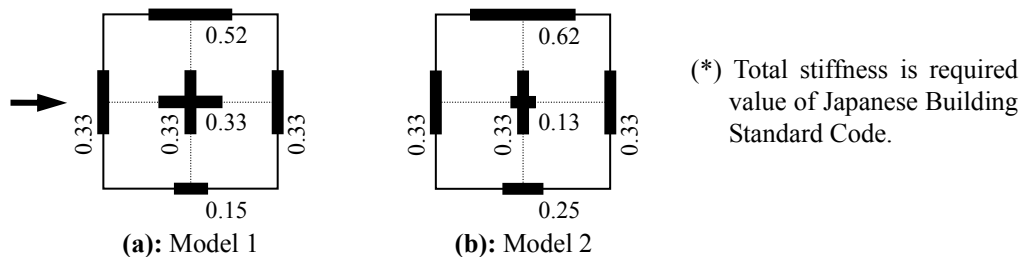


**Figure 6:** Balance of stiffness

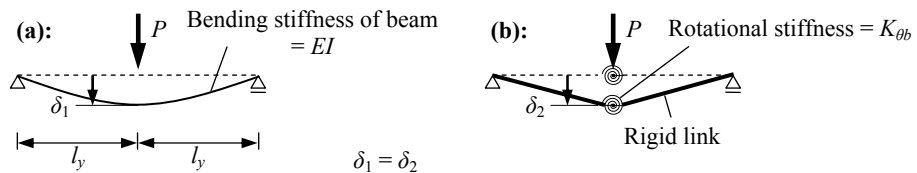


**Figure 7:** Procedure of determining stiffness of rotational spring

## 4. EVALUATION OF SEISMIC RESPONSE

### 4.1. Procedure of Evaluation

In this paper, two evaluation methods are used.

#### a) Spectrum Procedure

It is assumed that pseudo acceleration spectrum  $S_{pa}$  is constant and damping ratio of all modes are the same. Using SRSS method, maximum deformation of inner frame  $u_{x,\max}$ , flexible side frame  $u_{x1,\max}$ , stiff side frame  $u_{x2,\max}$  and orthogonal outer frame  $u_{y2,\max}$  are calculated as follows.

$$q_{i,\max} = \beta_i S_{pa} / \omega_i^2, \quad \beta_i = \phi_i^T \mathbf{m} \{1\} / \phi_i^T \mathbf{m} \phi_i \quad (4.1a,b)$$

$$u_{x,\max} = \sqrt{\sum_{i=1}^4 (\phi_{1i} q_{i,\max})^2}, \quad u_{x1,\max} = \sqrt{\sum_{i=1}^4 \{[\phi_{1i} + \phi_{2i}(l_y/r_m)] q_{i,\max}\}^2}$$

$$u_{x2,\max} = \sqrt{\sum_{i=1}^4 \{[\phi_{1i} - \phi_{3i}(l_y/r_m)] q_{i,\max}\}^2}, \quad u_{y2,\max} = \sqrt{\sum_{i=1}^4 [\phi_{4i}(l_x/r_m) q_{i,\max}]^2} \quad (4.2a-d)$$

Where,  $\phi_i, \beta_i$  = eigen vector and participation factor of  $i$ -th mode, respectively.

Similarly, maximum acceleration of each frame is evaluated as follows.

$$\ddot{u}_{x,\max} = \phi_{11} \omega_1^2 q_{1,\max}, \quad \ddot{u}_{x1,\max} = [\phi_{11} + \phi_{21}(l_y/r_m)] \omega_1^2 q_{1,\max}$$

$$\ddot{u}_{x2,\max} = [\phi_{11} - \phi_{31}(l_y/r_m)] \omega_1^2 q_{1,\max}, \quad \ddot{u}_{y2,\max} = \phi_{41}(l_x/r_m) \omega_1^2 q_{1,\max} \quad (4.3a-d)$$

In Eqn. 4.3, only 1st. mode is taken into account because of the reason described later.

#### b) Static Procedure (Conventional Procedure)

Generally, equally distributed lateral force is used for pushover analysis for 3-dimensional model even when floor diaphragm is not so stiff. Maximum displacement by this method is calculated as follows.

$$\mathbf{u}_{\max,s} = S_{pa} \mathbf{k}^{-1} \mathbf{m} \{1\} \quad (4.4)$$

$\mathbf{m}, \mathbf{k}$  and  $\{1\}$  are shown in Eqn. 2.14. This procedure assumes  $\ddot{u}_{x,\max} = \ddot{u}_{x1,\max} = \ddot{u}_{x2,\max} = S_{pa}$  and  $\ddot{u}_{y2,\max} = 0$ .

### 4.2. Results and Discussions

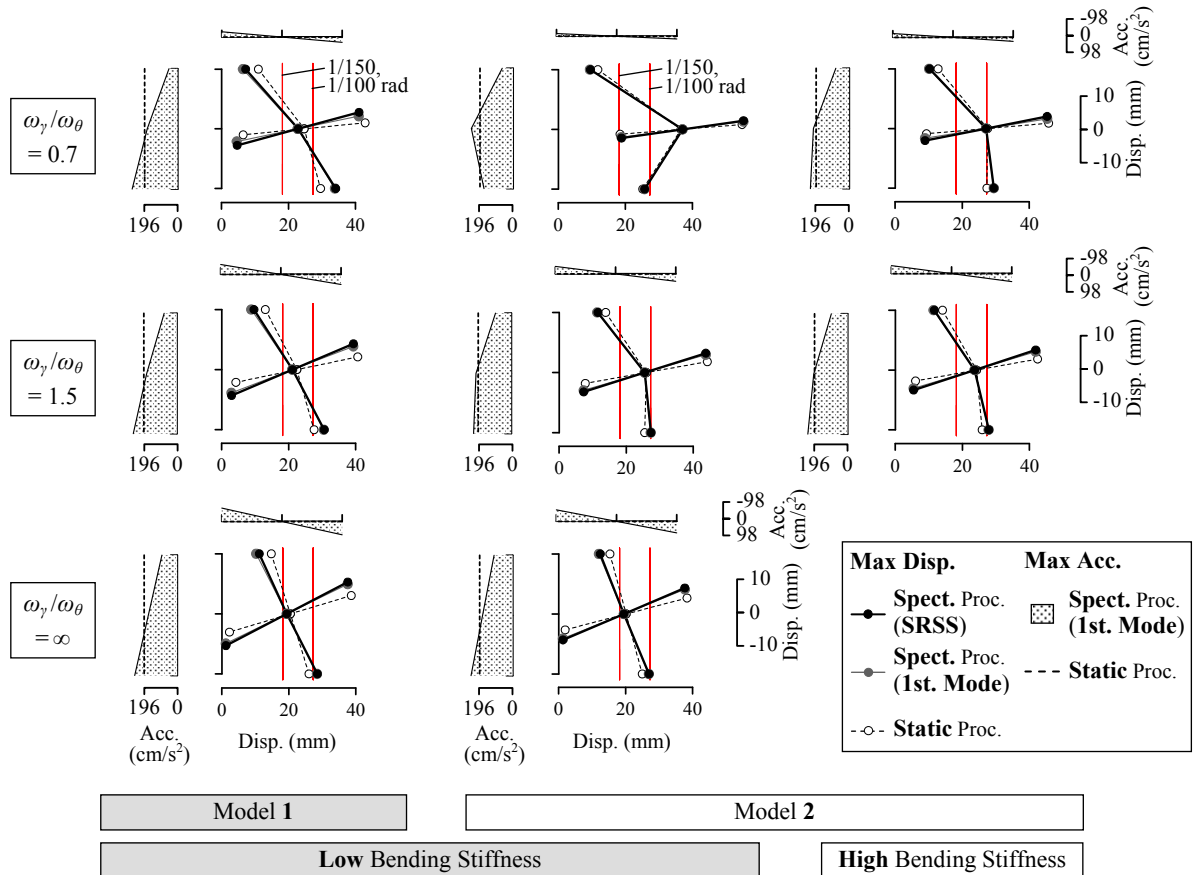
In this section, results from two procedures are compared. Spectrum method using SRSS method is likely to be accurate result, and accuracy of spectrum procedure considering only 1st. mode and static procedure are examined.

Figure 8 shows distribution of maximum displacement and acceleration of model 1 (low bending stiffness), model 2 (low bending stiffness) and model 2 (high bending stiffness). As for model 1, only "low bending stiffness" is examined because dynamic properties of model 1 are not so affected by bending stiffness.  $\omega_y/\omega_\theta = 0.7, 1.5, \infty$  and  $S_{pa} = 196 \text{ cm/s}^2$  are considered.

At first, it is found that the results of maximum displacement from spectrum procedure using SRSS method and 1st. mode are nearly the same. For this reason, when we conduct pushover analysis, distribution of external force should be similar to modal shape of 1st. mode. However, distribution

shapes of acceleration from spectrum procedure (1st. mode) and static procedure are quite different. Therefore, the reliability of static procedure seems to be a little lacked. Actually, the accuracy of static procedure is reduced in the case of model 1 while they are not so reduced in the case of model 2.

Secondly, maximum displacement of various  $\omega_\gamma/\omega_\theta$  is focused on. When  $\omega_\gamma/\omega_\theta$  is infinity, maximum displacement angle of flexible frame of all models are nearly less than  $1/100$  rad. However, the less  $\omega_\gamma/\omega_\theta$  is, the larger maximum displacement become. It is remarkable especially in the case of model 1 and model 2 (low bending stiffness). As we have pointed out in the previous research (2011),  $\omega_\gamma/\omega_\theta \geq 1.5$  seems to be reasonable criteria for rigid diaphragm, which means dynamic properties and seismic response are not so different from those of structures with infinitely rigid diaphragm.



**Figure 8:** Evaluation of maximum seismic response using spectrum procedure and static procedure

## 5. APPLICATION TO MULTI-SPAN STRUCTURE

### 5.1. Modification of Equation of Motion

If inner frame is eccentric, we can not use Eqn. 2.6 and 2.13. Therefore, modification of model and equation of motion is necessary. As shown in **Figure 9**, let  $pl_y$  and  $(2-p)l_y$  be the length of lower/upper areas in  $y$ -direction, respectively. In the previous chapters, we assumed  $p = 1$ .

Origin is set in the position as shown in **Figure 9** instead of  $c.m.$ . As a result,  $u_x$  is defined as displacement in origin. Therefore, Eqn. 2.6 is modified as follows.

$$\begin{aligned}
& \begin{bmatrix} m & p^2 m l_y / 4 & -(2-p)^2 m l_y / 4 & 0 \\ & p^3 I^{(x)} / 2 & 0 & 0 \\ & & (2-p)^3 I^{(x)} / 2 & 0 \\ \text{sym.} & & & I^{(y)} \end{bmatrix} \begin{Bmatrix} \ddot{u}_x \\ \ddot{\theta} + \ddot{\gamma}_{x1} \\ \ddot{\theta} + \ddot{\gamma}_{x2} \\ \ddot{\theta} - \ddot{\gamma}_y \end{Bmatrix} \\
& + \begin{bmatrix} K_x & -e_{y1} K_{x1} & -e_{y2} K_{x2} & 0 \\ & K_{\theta 1}^{(x)} + pGV/2 + K_{\theta b} & -K_{\theta b} & -pGV/2 \\ & & K_{\theta 2}^{(x)} + (2-p)GV/2 + K_{\theta b} & -(2-p)GV/2 \\ \text{sym.} & & & K_{\theta}^{(y)} + GV \end{bmatrix} \begin{Bmatrix} u_x \\ \theta + \gamma_{x1} \\ \theta + \gamma_{x2} \\ \theta - \gamma_y \end{Bmatrix} \quad (5.1) \\
& = \begin{bmatrix} m & p^2 m l_y / 4 & -(2-p)^2 m l_y / 4 & 0 \\ & p^3 I^{(x)} / 2 & 0 & 0 \\ & & (2-p)^3 I^{(x)} / 2 & 0 \\ \text{sym.} & & & I^{(y)} \end{bmatrix} \begin{Bmatrix} 1 \\ 0 \\ 0 \\ 0 \end{Bmatrix} \ddot{u}_g
\end{aligned}$$

Normalization of equation of motion like Section 2.4 is omitted.

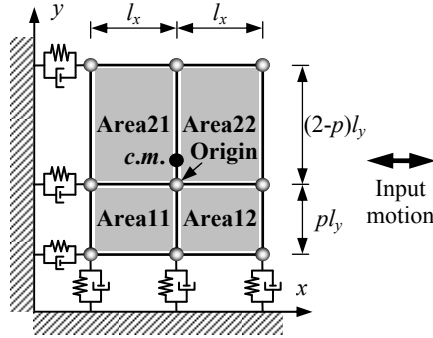


Figure 9: Generalized model (Inner frame is not located in the center)

## 5.2. Example Structure

In this section, Eqn. 5.1 is applied to multi-span structure more than 3-span. As shown in **Figure 10(a)**, the model of two spans in  $x$ -direction and four spans in  $y$ -direction are studied. This is modeled on the specimen of traditional timber house tested by Shimizu et al. (2010). Only mud walls are considered as stiffness element and floor stiffness is thought to be relatively low. The stiffness is identified from other tests. Natural period of the model is assumed to be 0.4 sec when the model has no stiffness eccentricity and floor diaphragm is rigid.

## 5.3. Verification of Adequacy

When the model is converted to reduced 2-span model, we can not determine where to locate inner frame. Therefore, three cases ( $p = 0.67, 1, 1.33$ ) are tried as shown in upper part of **Figure 10(b),(c),(d)**. By doing so, natural period and modal shape of 1st. mode are evaluated. These are compared with the results from eigen analysis of detailed frame model in lower part of **Figure 10(b),(c),(d)**. It is found that the model of  $p = 0.67$  shows good accuracy and its  $T_1$  is longest in all models.

As a result, we can conclude that dynamic properties of multi-span structure can be estimated by calculating those of a few reduced 2-span models. The model having longest  $T_1$  gives reasonable solution.

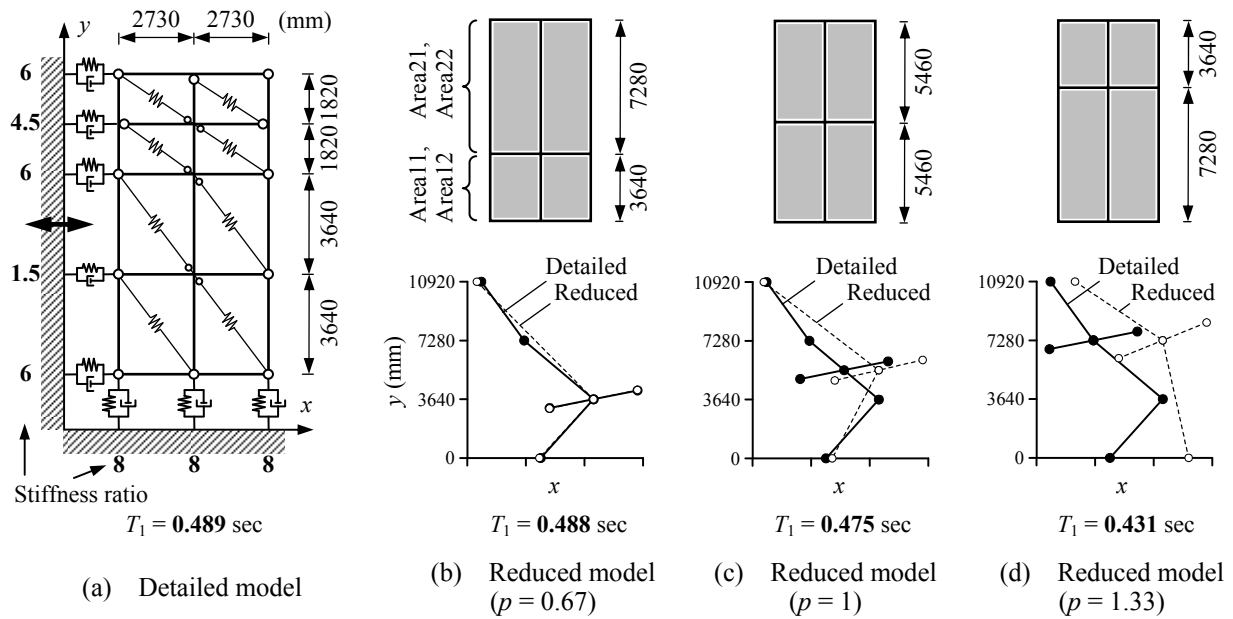


**Figure 10:** Estimation of modal shape and natural circular frequency of 1st. mode using reduced model

## 6. CONCLUSIONS

In this paper, reduced expression for timber structure with flexible floor diaphragm is presented. The findings of this research are as follows.

- 1) Equations of motion of a building with multiple discretized diaphragm elements are derived by defining reduced degrees of freedom.
- 2) In this model, not only shear stiffness of floor diaphragm but also bending stiffness of beams are taken into account. If shear stiffness of floor diaphragm is quite low, bending stiffness may affect dynamic properties.
- 3) Considering characteristics of typical timber houses, seismic response mainly derives from 1st. mode. Therefore, if pushover analysis for 3-dimensional model is conducted, we should consider not equal distribution of external force, which is typically used, but distribution similar to 1st. modal shape.
- 4) Proposed method is based on definition of 2-span structure. However, it can be applied to 3-span structure or over.

In this paper, linear structure is considered. However, equivalent linearization method based on this approach is likely to be effective for non linear structure. We will show the applicability in the future.

## REFERENCES

- Aoki, K., Tsuchimoto, T., and Ando, N. (2002), Effect of Shear Wall Configuration on Lateral Deformation of Conventional Japanese Timber Structures II, *Journal of the Japan Wood Research Society*, **48:6**, 439-448.
- Shimizu, H., Mukaibo, K., Horikawa, E., Tsuchimoto, T., Kawai, N., and Ohashi, Y. (2010), Study on Seismic Performance of Traditional Wooden Structure by Full Scale Shaking Table Tests, *Journal of Structural and Construction Engineering*, Architectural Institute of Japan, **75:657**, 2001-2008.
- Kawai, N. (2000), Application of Equivalent Linear Response Method Considering Shear Deformation of Horizontal Frames, *Summaries of Technical Papers of Annual Meeting Architectural Institute of Japan*, Architectural Institute of Japan, **C-1:Structures III**, 203-204.
- Yamazaki, Y., Kasai, K., and Sakata, H. (2011), A Basic Study on Dynamic Property and Seismic Response of Timber Structure with Flexible Floor and Uni-axial Stiffness Eccentricity, *Journal of Structural and Construction Engineering*, Architectural Institute of Japan, **76:663**, 959-968.